The MCD implies a symmetry assignment for the excited state of the transition. The symmetry assignment of $^3T_{2u}$ for this charge-transfer state and the implied placement of the πt_{1u} ligand orbital at higher energy than the πt_{2u} would be surprising except that the ordering of these orbitals has also been reversed by similar MCD studies of some of the 5*d* hexahalides.[24] There is the possibility that this reversal in the order of the ligand levels may be general. It is hoped that such MCD symmetry classifications will stimulate a theoretical consideration of these ligand orbitals.

It appears that MCD originating from a Jahn-Teller active ground state can be analyzed with reasonable success. The analysis presented is more complicated than that required for orbitally nondegenerate ground states, but it is hardly prohibitive. It might be possible to add second-order terms to the rotatory strength and the Zeeman interaction and to more precisely treat the data. However, the analysis presented appears to encompass the essentials of the problem.

ACKNOWLEDGMENTS

The experimental data presented here originated as a part of a doctoral dissertation presented to the Department of Physics and the Graduate School of the University of Oregon. The important contributions to this work that were made possible by that institution are gratefully acknowledged. Professor J. C. Kemp is thanked for initiating the author's interest in magneto-optics and for his sponsorship of the dissertation.

†Research sponsored jointly by ARPA through the Air Force Office of Scientific Research under contract with the University of Oregon (Contract No. 70-1912) and the U.S. Atomic Energy Commission under contract with the Union Carbide Corporation.

[1]R. G. Brabin-Smith and V. W. Rampton, J. Phys. C 2, 1759 (1969).
[2]F. A. Modine, thesis (University of Oregon, 1971) (unpublished).
[3]C. A. Bates, L. C. Goodfellow, and K. W. H. Stevens, J. Phys. C 3, 1831 (1970).
[4]T. Ray, Solid State Commun. 9, 911 (1971).
[5]T. Ray, Phys. Rev. B 5, 1758 (1972).
[6]R. Buisson and A. Nahmani, Phys. Lett. 37, 9 (1971).
[7]R. Buisson and A. Nahmani, Phys. Rev. B 6, 2648 (1972).
[8]S. N. Jasperson and S. E. Schnatterly, Rev. Sci. Instrum. 40, 761 (1969).
[9]D. D. Kasarda, J. E. Bernardin, and W. Gaffield, Biochem. 7, 3950 (1968).
[10]M. D. Sturge, Phys. Rev. 130, 639 (1962).
[11]R. W. Soshea, A. J. Dekker, and J. P. Sturtz, J. Phys. Chem. Solids 5, 23 (1958).
[12]H. H. Tippins, Phys. Rev. B 1, 126 (1970).
[13]D. S. McClure, Solid State Phys. 9, 400 (1959).
[14]D. L. Dexter, Solid State Phys. 6, 353 (1958).
[15]W. B. Fowler, *Physics of Color Centers*, edited by W. B. Fowler (Academic, New York, 1968).
[16]C. H. Henry, S. E. Schnatterly, and C. P. Slichter, Phys. Rev. 137, A583 (1965).
[17]C. H. Henry and C. P. Slichter, *Physics of Color Centers*, edited by W. B. Fowler (Academic, New York, 1968).
[18]A. D. Buckingham and P. J. Stephens, Ann. Rev. Phys. Chem. 17, 399 (1966).
[19]P. J. Stephens, J. Chem. Phys. 52, 3489 (1970).
[20]F. S. Ham, Phys. Rev. 138, A1727 (1965).
[21]J. S. Griffith, *The Theory of Transition Metal Ions* (Cambridge U. P., Cambridge, England, 1961).
[22]M. D. Sturge, Solid State Phys. 20, 91 (1967).
[23]M. J. L. Sangster and C. W. McCombie, J. Phys. C 3, 1498 (1970).
[24]S. B. Piepho, J. R. Dickinson, J. A. Spencer, and P. N. Schatz, J. Chem. Phys. 57, 982 (1972), and references therein.

PHYSICAL REVIEW B VOLUME 8, NUMBER 2 15 JULY 1973

Optical Properties of Mn^{2+} in Pure and Faulted Cubic ZnS Single Crystals

B. Lambert, T. Buch, and A. Geoffroy
Laboratoire de Luminescence II, Université de Paris VI-75005, Paris, France*
(Received 16 October 1972)

It is shown that a number of lines in the excitation and emission spectra of Mn^{++} in ZnS single crystals are associated with the presence of stacking faults in predominantly cubic crystals. The position of these lines is interpreted in terms of the modification of the cubic crystal field at the faulted sites.

I. INTRODUCTION

The optical properties of Mn^{++} and other impurities in ZnS host crystals have been studied rather extensively, especially due to the great interest in variously doped ZnS as synthetic phosphors, where Mn^{++} plays the role of an efficient activator.[1] The essential aspects of the absorption and emission

spectra of this ion have thus been well studied and understood, especially since independent studies of the phonon spectrum[2] of the crystals have confirmed the interpretation of most of the observed fine structure of the bands as phonon-assisted transitions.[3,4]

However, the features of these spectra associated with the crystallographic varieties of ZnS are less well understood. This is partially due to an incomplete understanding of the crystal structure of the varieties of the so-called "hexagonal" ZnS. Thus, it has been recognized only recently that most crystals thought to be wurtzite are in fact mixed polytypes with no wurtzite at all, and that most crystals thought to be purely cubic contain in reality relatively important densities of stacking faults and are thus partly "hexagonal."

"Axial" centers have been optically detected for various D-state ions Fe^{2+}, $3d^6\ ^5D$[5]; Cu^{2+}, $3d^9\ ^2D$[6,7]; and Cr^{2+}, $3d^4\ ^5D$[8] and their relations to stacking faults have been clearly recognized in the case of the F-state ions Co^{2+} $3d^7\ ^4F$ and Ni^{2+} $3d^8\ ^3F$.[9,10] For example, for Co^{++}[9] the transitions are $^4A_2 - {}^4T_1$, $^4T_2$ in absorption, and the features associated with hexagonality are comparable to those we observe for Mn^{2+}, $3d^5\ ^6S$. These authors suggest that a diminution in the cubic field[10] is responsible for the line shifts in their case but they do not interpret their spectra quantitatively, and their crystallographic model for the environment of an impurity ion located at a stacking fault neglects some important aspects of this environment.

The detection of two axial sites of Mn^{++} in ZnS with stacking faults by electron paramagnetic resonance[11,12] has led us to a detailed model for the impurity sites located at these stacking faults, and at the same time provoked in us healthy doubts about all affirmations of structural purity in ZnS. We therefore decided to reexamine the optical spectra of Mn^{++} in ZnS as a function of structure.

We were, in fact, able to detect in these spectra lines which are due to Mn^{++} in the two sites characteristic of the stacking faults. Using the results of a lattice-sum calculation of the crystal field parameters for these two sites, together with molecular-orbital theory, we are able to account for most of the supplementary lines which we observe in the faulty samples and which we can show to be absent in truly cubic crystals.

II. EXPERIMENTAL RESULTS

Excitation and emission spectra of our crystals have been obtained by means of a Jobin–Yvon HRS monochromator at liquid-helium temperatures.

Samples were synthetic single crystals doped during their growth. The cubic crystals were prepared by transport at relatively low temperatures.[13] The crystals containing stacking faults were extracted from a melt at high temperature and high pressure.[14] All crystals contained about 10^{-1}–10^{-2} at.% Mn per mole ZnS.

The density of stacking faults is measured by the degree of hexagonality α which has been estimated from measurements of birefringence.[11] The α coefficient may be defined as the percentage of planes which have hexagonal (prismatic) second-neighbor environment. It is to be noted that in Refs. 11 and 12 we talked about "mixed polytype" crystals. A polytype consists of a regular sequence of stacking faults. We do not have evidence that our crystals are true polytypes, and prefer, therefore, to speak about stacking faults. The distinction is completely irrelevant, as far as our results are concerned.

Figures 1–5 show the optical spectra obtained. In all the bands we studied, the effect of the stacking faults (SF) is clearly visible. This is in opposition to the results of Langer and Ibuki.[3] It is now doubtful that these authors ever experimented with a truly cubic crystal. In what follows we discuss the difference between cubic and faulty crystals in detail.

a. Absorption band at 21 500 cm^{-1} (4650 Å) (*Fig.* 1). This band corresponds to the transition $^6A_1 - {}^4E$. The transition $^6A_1 - {}^4A_1$ is not observed in this region of the spectrum. Calculations show[15,16] that the effect of covalency is sufficiently important to lift the degeneracy between ^4E and $^4A_1$ by at least 1000 cm^{-1}, and the transition probability is probably smaller to $^4A_1$ than to ^4E. The band at 21 500 $cm^{-1} = 21.5k$ K presents a well-resolved triplet of narrow lines, centered about 21 237 cm^{-1}, which is seen in all crystals (Fig. 2). The fine structure of this triplet is due to spin-orbit and spin-spin coupling.[16] The triplet comes from a pure electronic transition [zero-phonon line (ZPL)]. At the characteristic distance of 301 cm^{-1} corresponding to a local mode of the Mn^{2+} ion, we find the phonon-assisted transition at 21 538 cm^{-1}.[3,4] In the cubic crystals between these structures, there are only several wide bands which probably correspond to transitions associated with one or two acoustic phonons, TA, LA, and 2TA, whereas in the faulted crystals (Fig. 2), there appear two repetitions of the ZPL triplets, 14.9 and 86.5 cm^{-1} from the cubic ZPL. The intensity of these supplementary lines grows linearly with α. The relative intensity of the 14.9-cm^{-1} line is equal to α, whereas that of the 86.5-cm^{-1} line is somewhat larger. These "satellites" have already been described by Langer and Ibuki.[3] It is their absence in truly cubic crystals which is to be noted (Fig. 2).

b. Absorption band at 20 100 cm^{-1} (4980 Å). This band is assigned to the transition $^6A_1 - {}^4T_2$. The general appearance of this band in our crystals is like that of $^6A_1 - {}^4E$. In the cubic crystals one sees a ZPL at 19 684 cm^{-1} (5080 Å) split into a doublet 3 cm^{-1} apart (Fig. 3), a one-phonon sharp

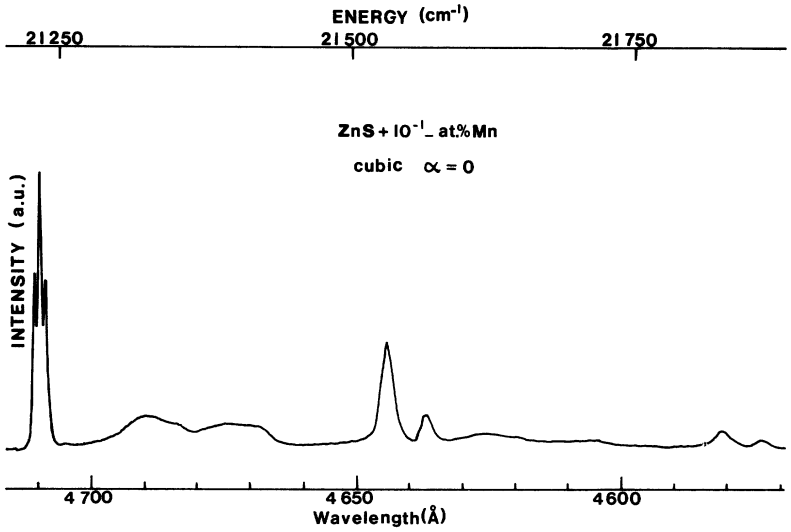

FIG. 1. Excitation spectrum of the absorption band $^6A_1 \rightarrow {}^4E$ in a pure cubic ZnS single crystal.

satellite at 300 cm^{-1}, and the wide acoustic-phonon bands between these lines. In the crystals with SF there is at 97 cm^{-1} a supplementary doublet whose splitting is 13 cm^{-1} (Fig. 3) and whose intensity grows with α. At higher resolution (Fig. 4) this doublet allows a third line to be seen. Measurements under polarized light show the components of this triplet to be polarized as shown (Fig. 4).

c. Emission band at 17 100 cm^{-1} (5860 Å). In cubic crystals this band shows a zero-phonon line at 17 899.3 cm^{-1} and a large band towards lower energy, on which several phonon lines 300 cm^{-1} apart from each other are visible, as well as the acoustic-phonon lines corresponding to the modes TA, LA, and 2TA. In the spectra of crystals containing stacking faults, there appear supplementary lines, displaced towards shorter wavelengths, whose relative intensity grows with α. This supplementary structure consists of a ZPL at 301.6 cm^{-1} from the cubic ZPL with its acoustic-phonon bands, which are, as always, rather broad, and of a second ZPL at 91.5 cm^{-1} (Fig. 5). Lines in this region were also reported by Lander and Ibuki,[3] who saw them in some of their crystals.

We have made no measurements on the other absorption bands, which were always either too weak or too ill resolved.

III. DISCUSSION OF EXPERIMENTAL RESULTS

Before we proceed to an explanation of the supplementary spectral lines associated with SF's in ZnS, we shall briefly discuss the crystallographic nature of these SF's. In opposition to some ideas frequently encountered, most "partially hexagonal" crystals of ZnS are not at all a sequence of zinc-blende and wurtzite regions, the latter hexagonal-close-packed structure being altogether absent from such crystals. Instead, a SF consists of a

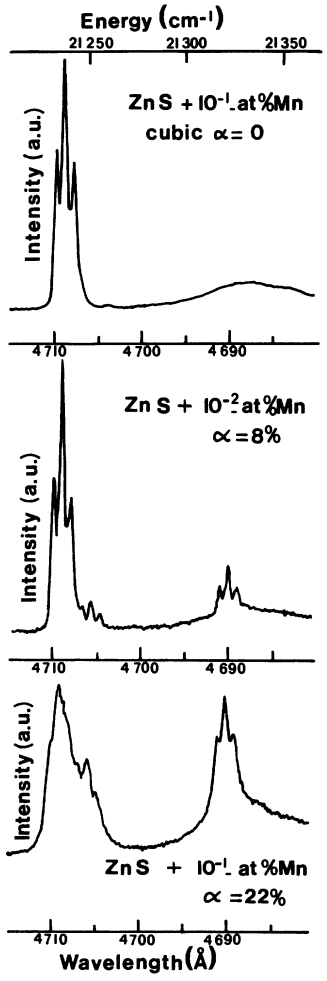

FIG. 2. Excitation spectra of the absorption band $^6A_1 \rightarrow {}^4E$ in a pure cubic ZnS single crystal and in cubic crystals with stacking faults ("hexagonality" coefficients $\alpha = 8$ and 22%).

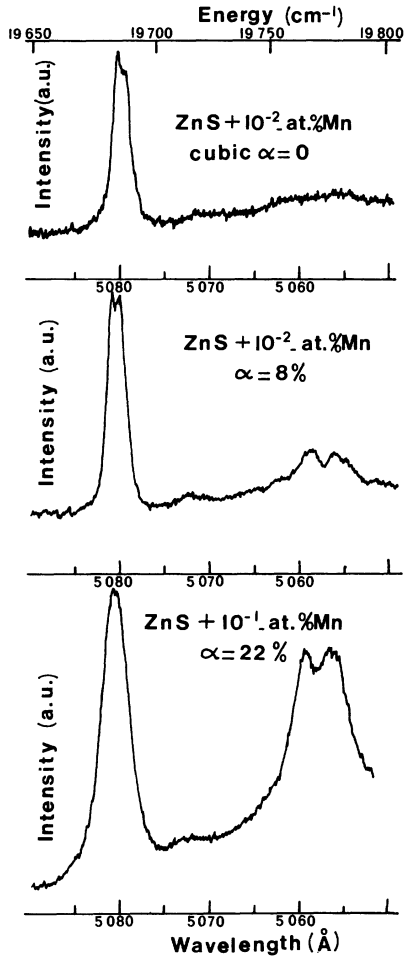

FIG. 3. Excitation spectra of the absorption band ${}^6A_1 \rightarrow {}^4T_2$ in a pure cubic ZnS single crystal and in cubic crystal with stacking faults ("hexagonality" coefficients $\alpha = 8$ and 22%).

sequence of two crystallographic planes possessing an axial structure different from wurtzite. In a previous publication[11] we have called these centers PN and AS, the wurtzite site being PS and the cubic one AN. In these double symbols, the couples P/A and S/N refer to the two outstanding features of the ionic distribution out to the third-nearest neighbors. The first neighbors of a given atom always form a tetrahedron, six of the second neighbors may form a trigonal prism (P) or antiprism (A), and a single third neighbor may be present (S) or absent (N). How these sites arise by different stacking schemes of the crystal planes has been explained in detail elsewhere.[11]

These crystallographic features determine the axial crystalline field parameters at any site. An S site possesses an axial field of the second power (which is absent in an N site) and an axial field of the fourth power. A P character is related to the appearance of an axial field of fourth power, and simultaneously modifies the cubic field. The crystal field relevant to our spectra is thus written

$$
\begin{aligned}
V &= V_{\mathrm{cub}} + V_{\mathrm{ax}} = \gamma_{40} Y_4^0 + \gamma_{43} \sqrt{\tfrac{1}{2}} (Y_4^3 - Y_4^{-3}) , \\
V_{\mathrm{cub}} &= V_{\mathrm{cub}}(\mathrm{AN}) + v_4 [Y_4^0 + \sqrt{\tfrac{10}{7}} (Y_4^3 - Y_4^{-3})] \\
&= \sqrt{\tfrac{7}{20}}\, \gamma_{43} [Y_4^0 + \sqrt{\tfrac{10}{7}} (Y_4^3 - Y_4^{-3})] , \\
V_{\mathrm{ax}} &= (\gamma_{40} - \sqrt{\tfrac{7}{20}} \gamma_{43}) Y_4^0 = \gamma_4 Y_4^0 .
\end{aligned}
\tag{1}
$$

It is seen in Table I that A sites (AN and AS) have slightly different cubic fields (2%), whereas the P sites clearly have stronger cubic fields. There are also modifications in the odd field (third power) which might affect the transition probabilities. Thus the third-order term is about 50% stronger for PN than for AS.[11]

If we now look at the position of the extra spectral lines associated with SF's (${}^6A_1 - {}^4E$ transition), we see that it is very tempting to assign the triplet at 14.9 cm^{-1} from the cubic (AN) line to AS and that at 86.5 cm^{-1} to PN. This leads us to postulate that the displacement is proportional to the cubic-field variation. As a matter of fact, this linear relationship is remarkably well satisfied for both triplets. An extrapolation of this procedure would allow one to predict the true wurtzite ZPL at 21 330 cm^{-1}. In fact, we did observe this line in wurtzite needles at 21 335.6 cm^{-1}.[17]

Theoretically this shift is not obvious. In fact,

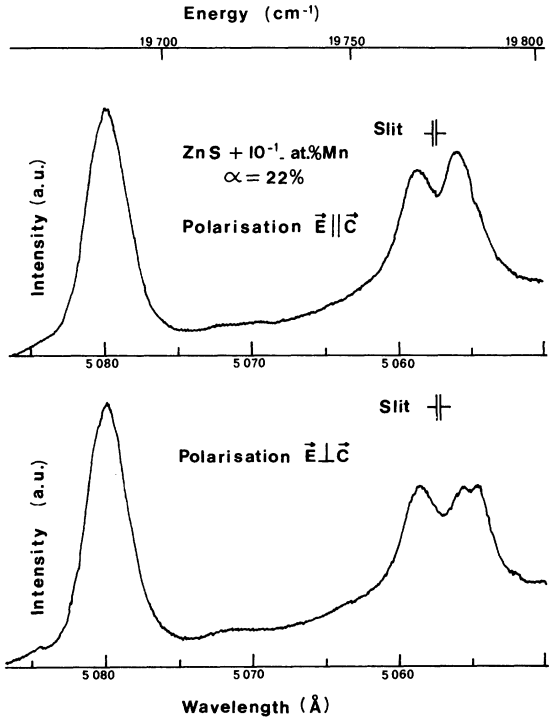

FIG. 4. Excitation spectra of the absorption band ${}^6A_1 \rightarrow {}^4T_2$ in a ZnS single crystal with stacking faults ($\alpha = 22\%$). Excitation light is polarized $\vec{E} \parallel \vec{C}$ and $\vec{E} \perp \vec{C}$.

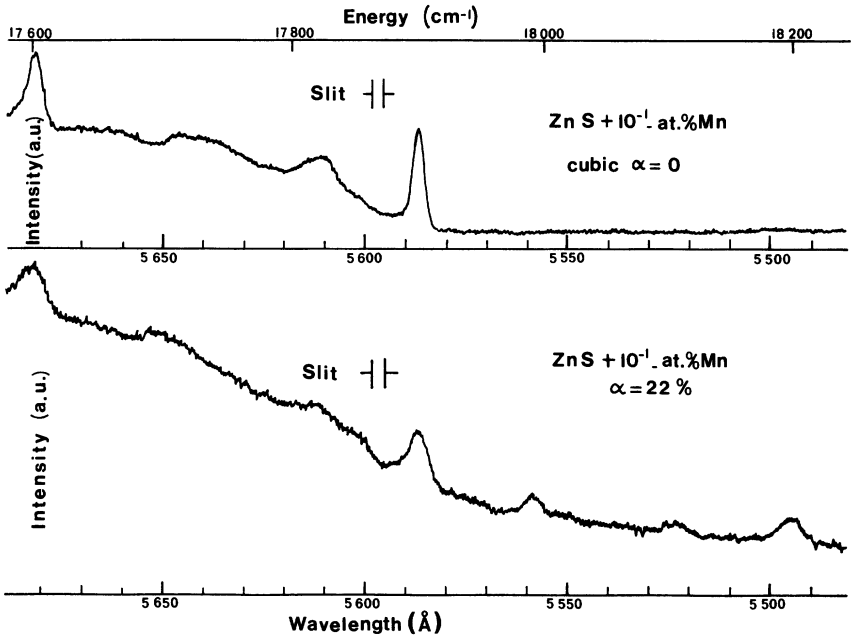

FIG. 5. Emission spectra of the band $^4T_1 \rightarrow {}^6A_1$ in a pure cubic ZnS single crystal and in cubic crystal with stacking faults ("hexagonality" coefficient $\alpha = 22\%$.) ZPL of axial centers are at 91.5 and 301.6 cm^{-1} towards the higher energies.

in the framework of a crystal field model, the ^4E level is completely independent of the cubic field; furthermore, a similar difficulty arises in the interpretation of the supplementary lines in the $^4T_2$ and $^4T_1$ bands. These lines are always shifted towards higher energies, whereas the levels should shift in the opposite direction when the crystal field increases.

We see thus that a simple crystal field model is unable to explain our effect. This is not surprising, since it has been shown that this theory fails to explain many details of the properties of transition-metal ions in partly covalent crystals. We propose therefore an explanation based on the idea that a change in the cubic crystal field produces a redistribution of the charge density between the impurity ion and the neighboring sulphur atoms (ligands). This redistribution can be calculated by molecular-orbital theory, and it will be seen that there are indirect effects on the position of the atomic levels of the impurity via covalency. We shall develop this idea in Sec. IV, and we shall see that it allows one to understand the spectra quite well.

IV. THEORY OF CUBIC-FIELD EFFECT

The total change in the energy E of a given level of the impurity center upon a change δq of the cubic crystal field q is expressed by means of the total derivative dE/dq. We take q to represent the purely ionic crystalline potential. δq has complex effects on the energy levels because it acts on the charge-density distribution over the pseudomolecule or cluster formed by the impurity ion and its neighbors. This distribution is measured by a covalency parameter x which describes the net relative electronic charge on the Mn ion. We make here the fairly rough approximation that a single covalency parameter is sufficient. We take x to be that of the antibonding $4t_2$ orbital, which has mainly Mn $3d$ character, with admixture of a few percent ligand σ function.

The splitting between the monoelectronic states $4t_2$ and $2e$ (respectively, antibonding σ and π functions) under the combined effect of the crystal field and charge transfer is defined to be the parameter Δ. In the presence of charge transfer, Δ is no longer necessarily proportional to q. The total derivative of Δ with respect to the crystal field is now

$$\frac{d\Delta}{dq} = \frac{\partial \Delta}{\partial q} + \frac{\partial \Delta}{\partial x}\frac{dx}{dq} \ , \tag{2}$$

whereas the simple crystal field theory gives only $d\Delta/dq = \partial\Delta/\partial q = \text{const}$. We shall calculate Eq. (2) by molecular-orbital theory, which yields directly the total derivative. One finds, however, that $d\Delta/dq$ is considerably smaller than $\partial\Delta/\partial q$.

The energy eigenvalues of the different quartet

TABLE I. Axial- and cubic-field parameters defined in Eq. (1). Units are atomic units $\times R^{l+1}$. The cubic field for AN is 1.10 in the same units.

	γ_2	γ_4	ν_4	$\sqrt{\frac{7}{20}}\gamma_{43}$
AN (cubic)	−0.0043	0	0	1.10
AS	−0.0563	−0.0534	+0.02	1.12
PN	−0.0041	+0.0891	+0.09	1.19
PS (wurtzite)	−0.0553	+0.0367	+0.10	1.20

TABLE II. Calculated displacements (in cm^{-1}) of spectral lines of the "axial" centers relative to the cubic-center line. This displacement is due to cubic-field effect.

	$^4T_1$	$^4T_2$	^4E
AS	+4 ± 20	20 ± 15	35 ± 10
PN	+10 ± 60	70 ± 40	130 ± 30
PS	+30 ± 80	90 ± 55	160 ± 40

levels, $^4T_1$, $^4T_2$, ^4E, $^4A_1$, which are the lowest excited states of our nominally $3d^5$ $^6A_1$ system, can be obtained through diagonalization of the corresponding electrostatic plus crystal field matrices, either in the weak-field or in the strong-field scheme.[18] In each case, the matrices depend on Racah's parameters B and C and on the splitting parameters Δ. Thus, $E = E(B, C, \Delta)$ for each level. But, as we have seen above, Δ depends on q and on the covalency $x = x(q)$, and both B and C depend on covalency through electron delocalization which modifies the electrostatic repulsion integrals. Therefore, the total derivative of E with respect to q is, for each level, given by

$$\frac{dE}{dq} = \frac{\partial E}{\partial \Delta}\left(\frac{\partial \Delta}{\partial q} + \frac{\partial \Delta}{\partial x}\cdot\frac{dx}{dq}\right) + \frac{dx}{dq}\left(\frac{\partial E}{\partial B}\frac{dB}{dx} + \frac{\partial E}{\partial C}\frac{dC}{dx}\right). \quad (3)$$

In this equation one simplification is implicit in the fact that only one x is used instead of at least two (x_σ and x_τ) and another is contained in the use of a single B, C, whereas here too several different parameters should be used, the general electrostatic parameters[19] $a, b, \ldots, j$ being the most general set. We take $B = B_0 x$, and thus $dB/dx = B_0$, which is the simplest choice, and a similar expression for C.

In order to obtain the partial derivatives $\partial E/\partial \Delta$, $\partial E/\partial B$, and $\partial E/\partial C$, we have performed numerical diagonalizations of the matrices of Tanabe and Sugano[18] (thus working in the strong-field scheme), after correcting these matrices for covalency effects in the simplified manner mentioned above. $\partial E/\partial B$ and $\partial E/\partial C$ are about equal for all three levels. This reflects the fact that the three levels have a very strong ^4G component common to all of them.

Varying B_0, C_0, Δ, and x systematically, we looked for the best fit between the calculated energies with those observed, viz., $17.89k$ K ($^4T_1$), $19.68k$ K ($^4T_2$), and $21.24k$ K (^4E). A fair agreement is obtained for $B_0 = (0.78 \pm 0.02)k$ K, $C_0 = (3.0 \pm 0.2)k$ K, $\Delta = (5.0 \pm 0.2)k$ K, and $x = 0.95 \pm 0.01$. The agreement is not very good. The best energies are $17.79k$ K, $20.11k$ K, and $21.12k$ K, respectively. Similar agreement can be reached for several sets of parameters. This explains the relatively large error margin on these.

The molecular-orbital calculation has been described before.[20] It yields the values $d\Delta/dq = 2.6k$ K and $dx/dq = 0.12$; dq is here expressed in units of the value q (AN) of the cubic center. In these units then $\delta q = 0.02$ for AS, 0.08 for PN, and 0.09 for PS. On the other hand, $\partial E/\partial \Delta = -0.8 \pm 0.1$ for $^4T_1$, -0.3 ± 0.05 for $^4T_2$, and zero for ^4E; $(\partial E/\partial B)(dB/dx) + (\partial E/\partial C)(dC/dx) = (17 \pm 5)k$ K for all three levels. We obtain the line displacements displayed in Table II for the three axial sites and the three levels.

The error margins shown in Table II are very large; this is due to the fact that following Eq. (3) the displacements are obtained as an (algebraic) sum of two contributions of opposite signs, each of which is affected by a large error.

V. COMPARISON WITH EXPERIMENT

A. Displacement Relative to Cubic Lines

If we now compare the results of our calculation with experimental results, we see that the agreement is quite satisfactory for both absorption bands. The theory renders the general appearance of both spectra in a semiquantitative manner. The displacements calculated for $^6A_1 - {}^4E$ are somewhat larger than those observed, but the proportionality to the cubic field is well reproduced, thus confirming our interpretation of these lines as being related to stacking faults.

The displacements calculated for $^6A_1 - {}^4T_2$ are somewhat smaller than those observed, if we assign the structure at about 90 cm^{-1} to the PN site. The displacement calculated for AS is about 20 cm^{-1}, but it might be only a few cm^{-1}. No line appears in this region when the hexagonality increases. However, it does not seem altogether impossible that this line might be hidden by the cubic line.

There is no agreement for the emission band $^4T_1 - {}^6A_1$. The extra lines seen in this band show displacements much too large when compared to theory, which predicts that the "axial" lines should be quite close to the cubic one, or even displaced towards longer wavelengths. This disagreement is not well understood at present. The largest displacement of 301.6 cm^{-1} is curiously close to the dominant phonon frequency of 297 cm^{-1}. This is surely just a coincidence.

B. Splitting of Lines

We must recognize the fact that the behavior of $^4T_1$ and $^4T_2$ is only partially understood at present both for cubic and axial lines. Particularly, the orbitally triply degenerate levels $^4T_1$ and $^4T_2$ should be split by the axial field of the axial sites, but the cubic lines of the same levels should likewise be split by spin-orbit coupling. A straightforward calculation gives for the spin-orbit splitting of $^4T_1$

a total splitting between the extremes of the four lines Γ_6, Γ_8, Γ_8, Γ_7 of about 50 cm^{-1}. The corresponding splitting is still larger for $^4T_2$. Nothing resembling such a splitting is observed on the "cubic" lines. On the other hand, similar values are calculated for the axial splittings of second and fourth power.

The symmetry of the orbital part of the spin-orbit coupling is T_1 and that of the axial field is T_2: Both could be quenched by a strong Jahn-Teller coupling to an E_g mode of vibration. If this hypothesis is correct, the effect of an uniaxial stress along the [111] axis of the crystals should be small, but that of an E_g symmetry stress, noticeable when stress is applied along [100] or [110], should not be quenched and therefore noticeable. Experimental results[21] seem to point in this direction and thus tend to confirm the hypothesis of a strong Jahn-Teller coupling to a tetragonal mode.

VI. CONCLUSION

As a consequence of the foregoing discussion we estimate that the main conclusions of the work presented here are (i) the positive experimental identification of the lines associated with the presence of stacking faults and polytypism in ZnS—this identification adds to the understanding of the optical spectra of Mn^{++} in these crystals; (ii) a confirmation of our model of the different impurity centers associated with these stacking faults and (at least semiquantitative) the validity of our calculation of the crystal field components of these centers.

---

*Equipe de recherche associée au Centre Nationale de la Recherche Scientifique.

[1]See, for example, *Physics and Chemistry of II-VI Compounds* (North-Holland, Amsterdam, 1967), Chap. 9.

[2]J. Bergsma, Phys. Lett. A **32**, 324 (1970).

[3]D. Langer and S. Ibuki, Phys. Rev. **138**, A809 (1965).

[4]R. Beserman and M. Balkanski, Phys. Status Solidi B **44**, 535 (1971).

[5]G. A. Slack, F. S. Ham, and R. M. Chrenko, Phys. Rev. **152**, 376 (1966).

[6]I. Broser and M. Maier, J. Phys. Soc. Jap. Suppl. **21**, 254 (1966).

[7]A. Suzuki and S. Shionoya, J. Phys. Soc. Jap. **31**, 1759 (1971).

[8]J. T. Vallin, G. A. Slack, S. Roberts, and A. E. Hughes, Phys. Rev. B **2**, 4313 (1970).

[9]S. A. Kazanski, A. I. Ryskin, and G. I. Khil'ko, Fiz. Tverd. Tela **10**, 2415 (1968) [Sov. Phys.-Solid State **10**, 8 (1969)].

[10]A. I. Ryskin, L. A. Sysoiev, and G. I. Khil'ko, Fiz. Tverd. Tela **14**, 911 (1972) [Sov. Phys.-Solid State **14**, 779 (1972)].

[11]T. Buch, B. Clerjaud, B. Lambert, and P. Kovacs, Phys. Rev. B **7**, 184 (1973).

[12]B. Lambert, T. Buch, and B. Clerjaud, Solid State Commun. **10**, 25 (1972).

[13]H. Samelson, J. Appl. Phys. **33**, 1779 (1962).

[14]Eagle-Picher Industries, Inc., Miami, Okla.

[15]S. Koide and M. H. L. Pryce, Philos. Mag. **3**, 607 (1958).

[16]C. Blanchard and R. Parrot, Solid State Commun. **10**, 413 (1972).

[17]B. Lambert, T. Buch, A. Geoffroy, and P. Kovacs, Solid State Commun. **12**, 147 (1973).

[18]Y. Tanabe and S. Sugano, J. Phys. Soc. Jap. **9**, 753 (1954).

[19]J. S. Griffith, *The Theory of Transition Metal Ions* (Cambridge U.P., London, 1961).

[20]T. Buch and A. Gelineau, Phys. Rev. B **4**, 1444 (1971).

[21]R. Parrot (private communication).